Self-locking Underactuated Mechanism for Robotic Gripper*

Jui Hsu[1,2], Eiichi Yoshida[2,1], Kensuke Harada[3] and Abderrahmane Kheddar[2,4]

***Abstract*— We describe the concept and first prototype of a novel mechatronic design of a robotic gripper, which aims at being mounted on a humanoid robot to achieve firm (i.e. locked) and robust grasps. Such grasps could ideally support complex multi-contact motions, such as ladder climbing, or manipulation of complex tools, with energy efficiency. For this purpose, we propose a solution by designing a smart self-locking underactuated mechanism mounted in parallel to actuators to be triggered automatically when the desired grasp is achieved. This design leverages adjustable power distribution between the gripper and the brake through a differential gear. The advantages of adaptive, firm grasping, and energy-saving capabilities of our gripper are experimentally demonstrated by a prototype gripper.**

I. Introduction

Humanoid robots are considered to be a solution to many applications thanks to their multi-functionality and adaptability to human workspace. They are expected to serve as manufacturing robots to perform tasks in large-scale manufacturing yards (such as aircraft, building, ships, etc.) under the supervision of a small number of human workers. Moreover, the DARPA robotics challenge boosted the idea that they can intervene in disaster situations to achieve preliminary reparations or monitoring operations. In such cases, there are needs to investigate whole-body motion and manipulation using multi-contact loco-manipulation. When climbing ladders, or when negotiating displacements in confined environments, the end-effectors or robotic grippers of the humanoid are used to support motions. Like our hands, they need to grasp and handle objects firmly when needed. Sometimes they should even support the body for tasks and multi-contact displacements. However, because of the weakness or lack of dexterity of current humanoid robot grippers, the environments where multi-contact behaviors can be fully applied are still limited [1].

Although there are already many robotic hands developed, their capability and reliability have still some room for improvement. An ideal hand designed for humanoid robots must at the same time (i) support large part of the weight of the robot, (ii) manipulate less heavy tools, (iii) be light, and (iv) be energy efficient. The tools or the environments may have complex geometry, both bilateral grasps and unilateral contacts of the hand are required.

*This research has partly been supported by the CNRS-AIST-AIRBUS Joint Research Program and JSPS Grant-in-Aid for Scientific Research (B) 16H02886 .

[1]University of Tsukuba, Tsukuba, Japan
[2]CNRS-AIST JRL (Joint Robotics Laboratory), UMI3218/RL, Tsukuba, Japan
[3]Osaka University, Osaka, Japan
[4]CNRS-UM LIRMM, Interactive Digital Humans, Montpellier, France

In this paper, a "self-locking underactuated mechanism" (SLUM) is devised to passively lock the gripper in the case of bilateral or even in some unilateral grasps. Utilizing the concept of underactuation and frictional locking, a power transmission is added to perform driving and locking with a small number of actuators. A prototype is designed and built to assess this new approach.

In section II, we briefly explore the background of the robotic hands and grippers. In section III, the concept of self-locking underactuated mechanism is explained in detail. Section IV presents a prototype, including the mechanical design, the analysis, and the experiment results. We then conclude our work with some future directions.

II. Related work on robotic grippers

There are a large variety of robotic grippers (hands) that differ in kinematics, motion capabilities, and mechanical design [2]. For example, by imitating the human hand kinematics and applying miniaturized actuators for each joint, several dexterous hands have been developed [3]. Their recognizable appearance and capability of interaction make them useful in prosthetics and fine manipulations. The problems of these highly actuated robotic hands are the overall size and the complexity due to the wiring. In order to simplify the control and save space, another approach is reducing the number of actuators by exploiting synergies or the application domain. For some industrial applications, the main task is to pick and place objects, the gripper can be of customized design. By simplifying the kinematic structure, many hands/grippers with less functional capabilities have been developed [4].

A. Adaptive couplings

By assigning an adaptive mechanical coupling in each joint, the complex control strategies can be simplified and the embedded sensors reduced. This self-adaptive mechanism is commonly called underactuation. A system is underactuated if the number of actuators is less than its degrees of freedom (DoF). An example of underactuated finger enclose an object

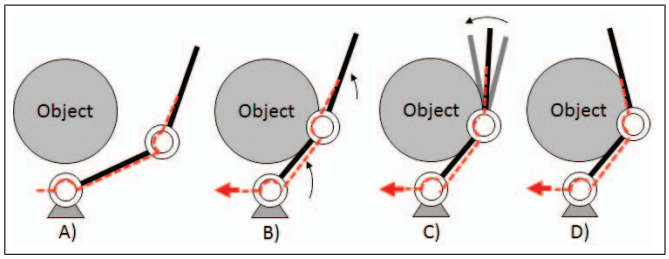

Fig. 1. Underactuated finger enclose process

is shown in Fig. 1 to illustrate the concept. When the object is fully grasped, the force applied at the actuator is distributed among the phalanges. This mechanism provides autonomous shape adaptation and force distribution on grasped objects.

Practically, a few underactuated robotic hand using different component have been proposed. For example, a linkage underactuated finger is given in [5]. In this work, a static analysis is applied to find the proper parameters for the geometric design of the finger. By introducing the underactuation among fingers with a differential gear, a 10-DoF hand driven by two actuators is devised. Another underactuated hand based on tendon is given in [6]. This hand has 19 joints and only uses one actuator to activate all of them. The adaptive synergy with novel mechanical design result in soft and safe, yet powerful and robust structure.

Furthermore, some work exploits rapid prototyping to make a low-cost platform for research purposes. In [7], an open-source 3D printed hand is made. A breakaway clutch mechanism is invented to provide underactuation without differential. In [8], a pulley-tendon underactuated eight DoF hand have been developed. A compliant joint is constructed, in comparison with the regular pin-joint.

B. Locking devices

High grasp force is an important subject for robotic grippers. In [9], a hand with very high fingertip force capabilities has been developed. This hand uses a hybrid transmission with gear and toggle mechanism to accomplish high force and speed in the same time.

On the other hand, there are many robotic systems that use external locking devices, see [10]. Mechanical lock, i.e. ratchets, usually has low energy consumption and compact size. Their locking ability is strong, though the variety of their locking positions is limited. In [11], a flexible gripper with a locking mechanism, consist of latch, magnets, and a SMA actuator. In contrast, friction lock normally has infinite locking positions. The locking ability is controllable but limited by the normal force. In [12], self-amplifying brakes are put in each joint of the gripper to perform certain grasps.

In robotic hands, non-backdrivable mechanisms, i.e. worm gears, are widely used due to their high reduction ratio and self-lock property. An innovative miniaturized, clutching mechanism is presented in [13]. The concept is assessed with a prosthetic hand prototype and an experimental product [14].

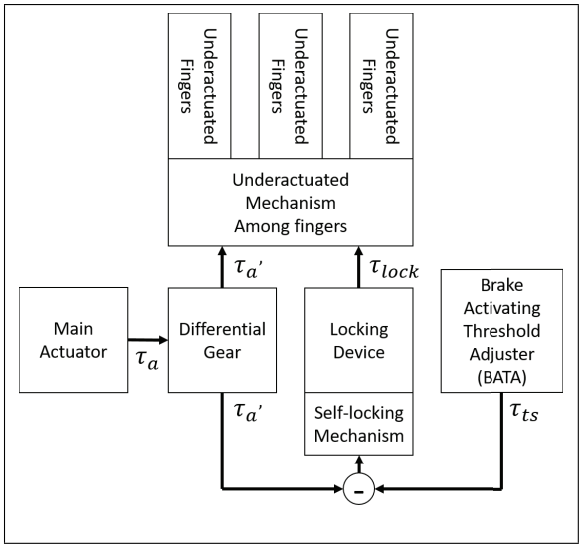

Fig. 2. Composition of SLUM

III. Self-locking underactuated mechanism

The self-locking underactuated mechanism (SLUM) we propose is based on combination of the shape adapting couplings and energy-saving lock together. Although there are other works involving underactuated finger and joint lock, in most cases the lock is passive or is driven by individual actuators. The passive lock lacks the backdrivability, which is a helpful feature for robotic hand in certain situations. Also, the reliability of using the non-backdrivable mechanism as the only locking device is questionable. As to the independent active lock, the timing of activating the lock is hard to determine without sensing. Moreover, adding actuators and sensors to the hand complicates the system and conflicts with the idea of underactuation.

We introduce a mechanical design to lock the hand when firmly grasping and keep the backdrivability of the hand otherwise. This feature reduces the collision damage by the unexpected contact between robot and the environment. The basic composition and the working procedure of SLUM is shown in Figs. 2 and 3. The underactuated hand is driven by the power of the main actuator through the differential gear terminal A and is locked by the locking device. Notice that this underactuated hand has only one input, which is connect to both differential and locking device by transmission.

For a given object, the configuration of the finger at any time is determined. After the grasp is completed, the contact force increases with the input torque τ_a. We make the assumption that the grasping force has a linear relationship with the input. For an object with known geometric data, we can easily evaluate the main actuator torque τ_a for a stable grasp.

Moreover, an active locking device which generates brake torque τ_{lock} is present. A brake activating threshold adjuster (BATA) is placed parallel to the input from the main actuator. This adjuster can be built by combining some passive mechanical element and a miniaturized actuator.

We can set a certain value of the torque generated by BATA as the threshold of the brake τ_{ts}. When the torque from differential gear terminal B, which has the same value as the input to hand, overcomes the threshold, the mechanism starts to move and the locking device is activated. By setting the proper value of the threshold, the hand will perform a grasp and will be locked automatically. A self-lock non-backdrivable mechanism is able to free the actuators from generating the power to maintain the current grasp state.

In Table I, we list some combination of the relative works along with the SLUM hand. The estimated performance in each item is compared, in order to clarify the contribution of this concept and also provide the design principle.

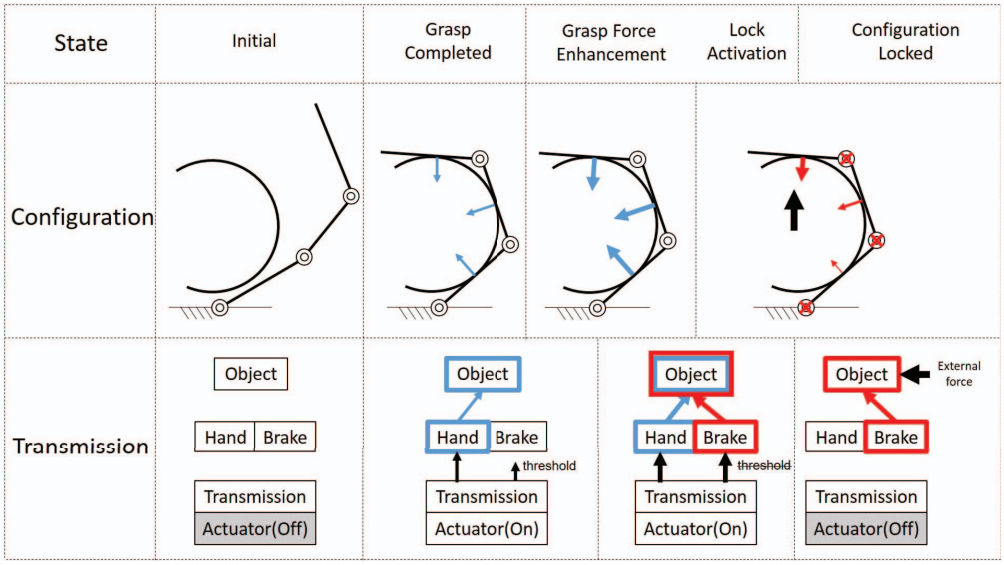

Fig. 3. Working procedure of SLUM

TABLE I

THE COMPARISON BETWEEN SLUM AND OTHER HANDS

Mechanical design	Speed torque ratio	Energy consumption	Back drivability	Unlock under high payload	Sensing requirement
Full-actuated hand with non-backdrivable transmission[14]	Low	High	No	Easy	High
Underactuated hand with non-backdrivable transmission[4]	Low	Low	No	Easy	Low
Underactuated hand with active mechanical lock[12]	High	High	No/Yes (Switchable)	Hard	Medium
Proposed SLUM hand	High	Low-Medium	No/Yes (Switchable)	Easy-Medium	Low

TABLE II

GRIPPER SPECIFICATION

Specification	Ideal gripper for humanoid	Presented prototype
Payload	25kg	10kg
Weight	3kg	3.5kg
Cross-section area	150mm x 120mm	250mm x 130mm
Height	240mm	300mm
Peak power	36W	30W

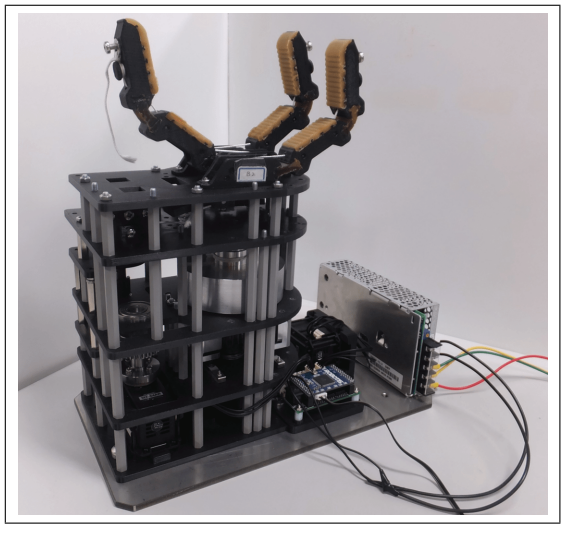

Fig. 4. The prototype: SLUM gripper

IV. PROTOTYPE: SLUM GRIPPER

A. Design

In order to verify the potential of SLUM, a prototype gripper is developed (shown in Figs. 4 and 5). To determine the design parameter of this prototype, we take other robotic grippers and the human body as references. For example, maximum payload should over 25kg to support a humanoid robot (about 45kg) with two hands. In Table II, we list some ideal specification and the measured specification of our first prototype.

The prototype gripper use two actuators (Dynamixel MX-64AR) to drive the gripper and adjust the brake threshold of the locking device. The composition of the finger module and its mechanism are shown in Figs. 7 and 8. The underactuated finger has compliant joints, made by urethane rubber, which acts as returning spring. The basic design refers to [15]. In [16], the stiffness in each joint is evaluated. It suggests that the value of the stiffness affects the force required to change

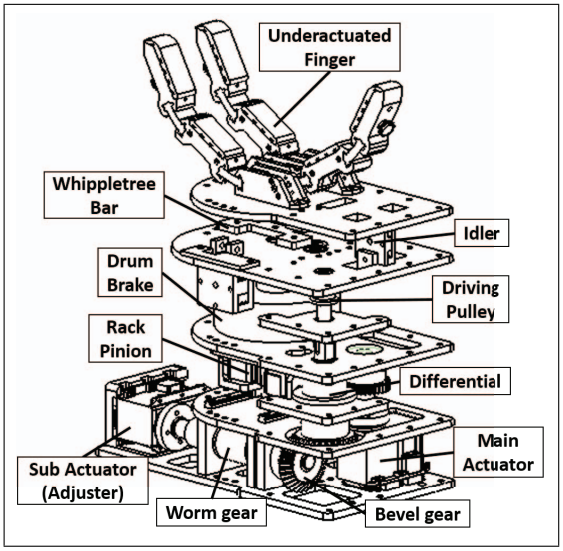

Fig. 5. The CAD model of the SLUM gripper

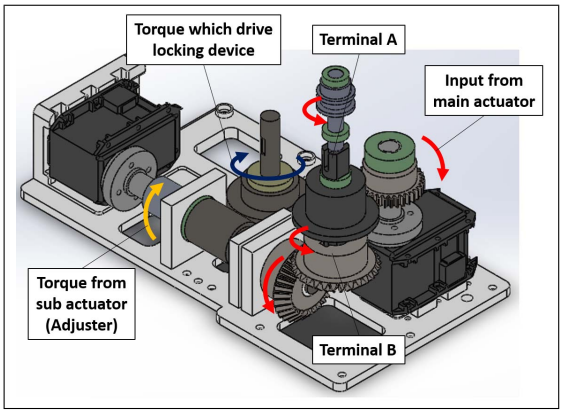

Fig. 6. BATA

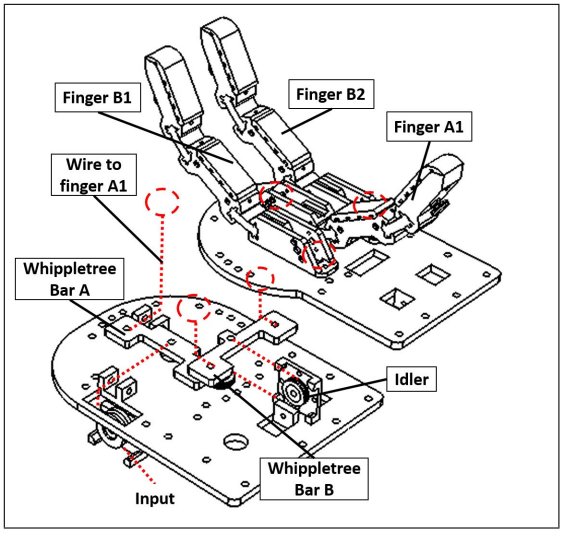

Fig. 7. Composition of the finger module

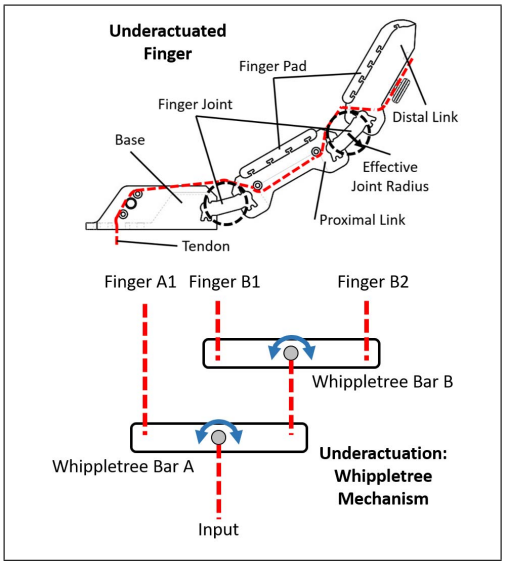

Fig. 8. The finger module mechanism

the configuration and that the ratio of the stiffness of each joint influences the range of the object size for stable grasp. All wires inside the three fingers are underactuated with a whippletree mechanism to increase the shape adaptability.

A miniaturized drum brake is adopted for both power density and manufacturing cost reason. The structure of the brake is shown in Fig. 9. Inside the drum, the brake shoes are pivoted on the structure base and cover by lining in the side that close to the drum. The drum, brake shoe and driving frame are made by aluminum alloy and the lining is made by cast iron for the strength and the coefficient of friction. A rack and pinion mechanism with module 1.5 is adopted, replacing the hydraulic cylinder in regular drum brake to push the shoe into the drum and generating friction force. A worm gear is added to enlarge the actuation force and make the locking device non-backdrivable.

B. Analysis

1) Underactuation: We simplify the model of underactuated system and use a numerical analysis to evaluate the capability of enduring the external force when the gripper is locked. We work with the following assumptions to analyze this amount:

- During the grasp, the object does not move and has no deformation either;
- The external force is applied in the normal direction of the palm of the gripper;
- The gripper consists of symmetric two phalanges fingers, and the transmit ratio of torque in each joint is known;
- The object has a cylindrical shape, and the center of mass of the object is on the center plane of the gripper.

Under these assumptions, the grasp posture and the position of the contact points can be obtained by the geometric analysis for certain object position.

If the grasping is successful, the contact forces and external force are balanced on the object, as shown in Fig. 10. In this state, the vector of each force can be estimated by the

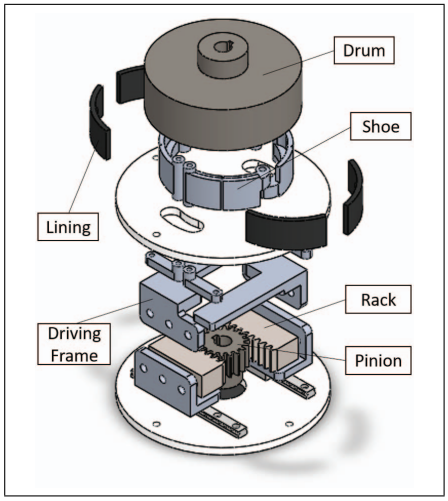

Fig. 9. Exploded-view of the drum brake

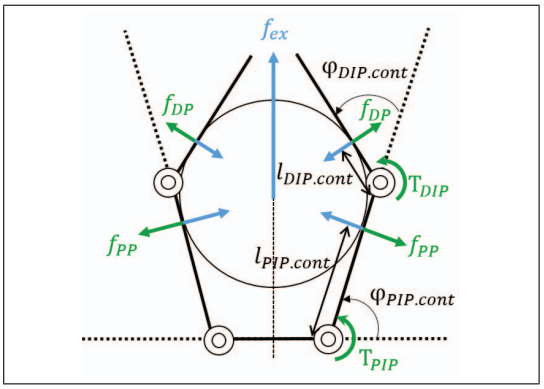

Fig. 10. Force balance

following equations:

$$f_{\mathrm{DP}} \times l_{\mathrm{DIP.cont}} = T_{\mathrm{DP}}(\tau_{\mathrm{fin}}, \phi_{\mathrm{DIP.cont}}) \tag{1}$$

$$\begin{aligned}(f_{\mathrm{DP}} \cos \phi_{\mathrm{DIP.cont}}) \times [l_{\mathrm{PIP.cont}} + (l_{\mathrm{DIP.cont}} \cos \phi_{\mathrm{DIP.cont}})] \\ + f_{\mathrm{PP}} \times l_{\mathrm{DIP.cont}} = T_{\mathrm{PIP}}(\tau_{\mathrm{fin}}, \phi_{\mathrm{DIP.cont}})\end{aligned} \tag{2}$$

$$\begin{aligned}f_{\mathrm{ex}} = 2 f_{\mathrm{DP}} \cos(\phi_{\mathrm{PIP.cont}} + \phi_{\mathrm{DIP.cont}} - \pi) \\ + 2 f_{\mathrm{PP}} \sin(\phi_{\mathrm{PIP.cont}} - \pi/2)\end{aligned} \tag{3}$$

where f is the contact force, f_{ex} is the external force, l is effective lever length of each force, T is the torque apply to the joints, τ_{fin} is the input torque to the finger, $\phi_{\mathrm{.cont}}$ is the degree of each joint when contact happened. The subscript text defines the following: DP as the distal link, DIP as the distal inter-phalangeal joint, PP as the proximal link, PIP as the proximal inter-phalangeal joint.

2) Drum brake: For designing a reliable locking device with compact size, the relationship between the geometric parameter and the brake torque is necessary. In [17], the basic property of the drum brake including self-energizing and de-energizing is explained in detail. A set of equations are derived and listed to evaluate the performance of the drum brake. The top view of the drum brake and its schematic

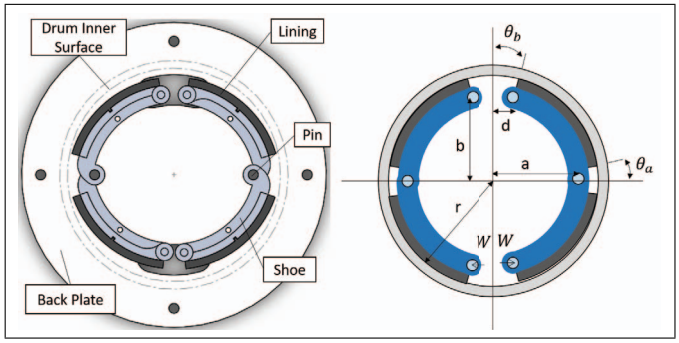

Fig. 11. Design parameter of drum brake

are shown in Fig. 11, to define the parameter. For the self-energizing shoe, the normal contact force moment is

$$M_{\mathrm{Ps}} = \frac{\mathrm{p}_{\max,s}}{4 \sin \theta_c} [2(\theta_c - \theta_a) \frac{\pi}{180^\circ} - \sin 2\theta_c + \sin 2\theta_a] \tag{4}$$

The friction moment is

$$\begin{aligned}M_{\mathrm{Fs}} = -\frac{\mu p_{\max,s} r t}{\sin \theta_c} \\ \times [r(\cos \theta_c - \cos \theta_a) + \frac{a}{2}(\sin^2 \theta_c - \sin^2 \theta_a)]\end{aligned} \tag{5}$$

where

$$\theta_c = 90^\circ - \theta_b \tag{6}$$

t is the shoe face width, μ is the coefficient of friction, $p_{\max,s}$ is the maximum contact pressure of the self-energizing shoe.

The actuation force to push both the self-energizing and deenergizing shoe is

$$W_s = W_d = \frac{M_{\mathrm{Ps}} - M_{\mathrm{Fs}}}{b} \tag{7}$$

The braking torque for each self-energizing shoe is

$$T_s = \frac{\mu p_{\max,s} r^2 t (\cos \theta_a - \cos \theta_c)}{\sin \theta_c} \tag{8}$$

Likewise, the braking torque for each deenergizing shoe is derived from eqs. (4)–(7) replacing $p_{\max,s}$ with $p_{\max,d}$. The total braking torque of the four shoes can be estimated.

The trade-off between the size and the capacity of the drum brake is an essential issue in the design process. We chose the inner diameter as the crucial factor for the drum brake, other parameters are decided from a linear relationship with the diameter and a numerical analysis is applied using `MATLAB`. As a result, an 84mm inner diameter drum with brake torque of 20.78Nm is determined.

C. Experiments

In Fig. 12, we show that many objects can be grasped and held by SLUM gripper as a preliminary test of the underactuated mechanism. A successful grasp is defined by more than 4 surfaces of the finger contacting the object and lifting the object against its own weight. Cylindrical objects with radius ranging from 20–50mm can be easily grasped for a wide range of initial positions. For the object with radius less than 20mm, the fingers can form a closure, preventing

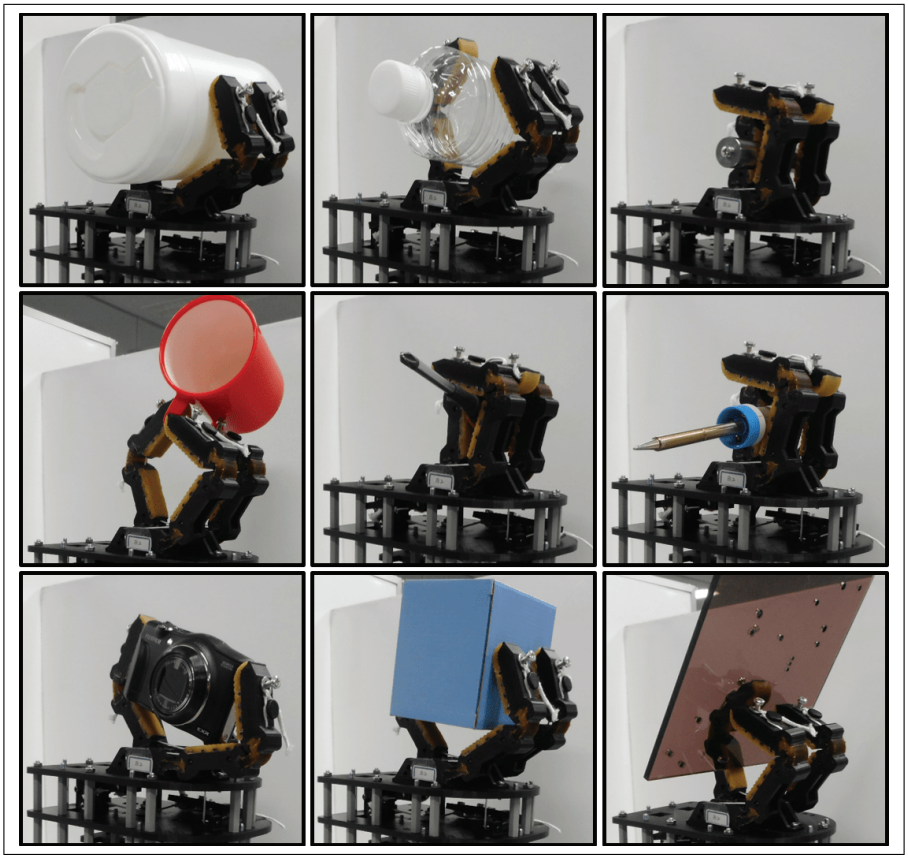

Fig. 12. Shape adaptability

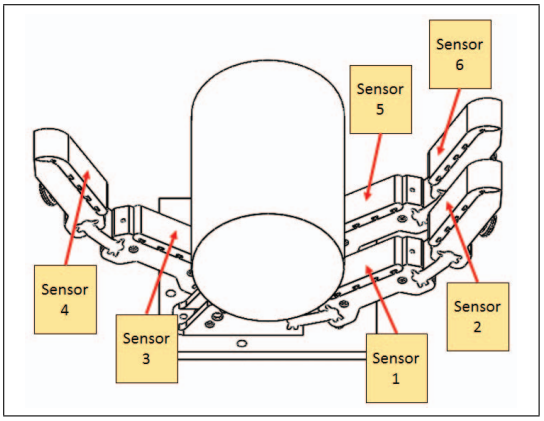

Fig. 13. Composition of the pressure sensors

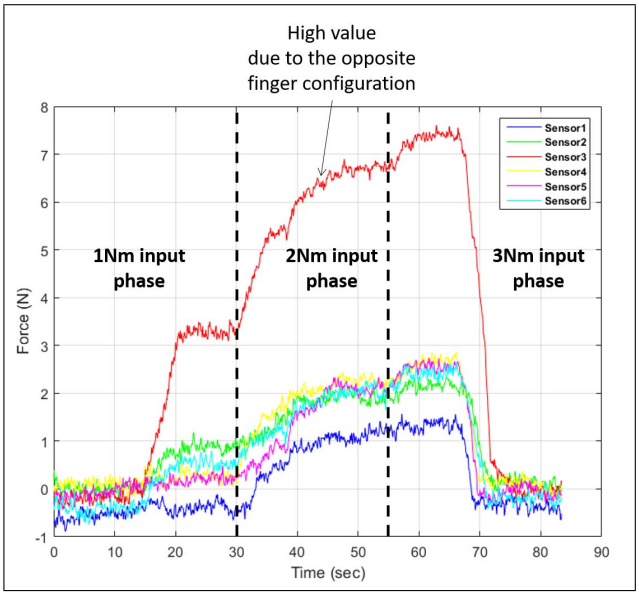

Fig. 14. Total contact force of all sensor

the object from slipping out the gripper. For a plate or more complicated objects, a pinch grasp can be achieved if we start from an adequate initial configuration.

In order to check the design parameters and confirm the relationship between the input torque and the grasp force, another test is made. The fingers grasp a cylindrical object placed within the gripper with different torque inputs from the actuator. In the whole process, a pressure sensor is attached to each phalanx of the finger to measure the contact pressure (see Fig. 13). This experiment is repeated three times; one of the result is shown in Fig. 14. As we expected, while the input torque increasing from 1Nm to 2Nm and 3Nm, the total force on each phalanx shows a stepwise diagram (sensor 3 –attached to the finger that is opposite to the other two, shows a higher resulting contact force). This verifies the positive correlation between the input torque

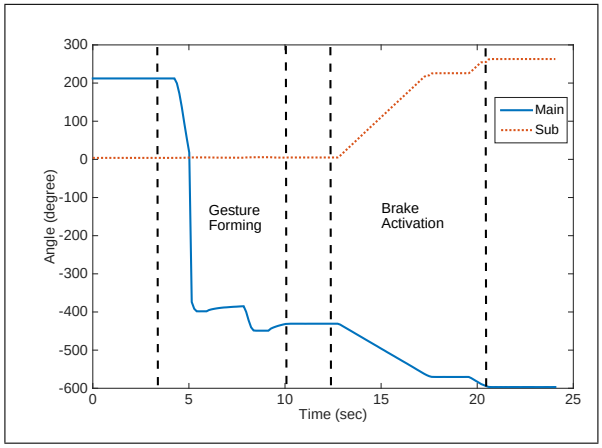

Fig. 15. Position value of two actuators in grasping locking process

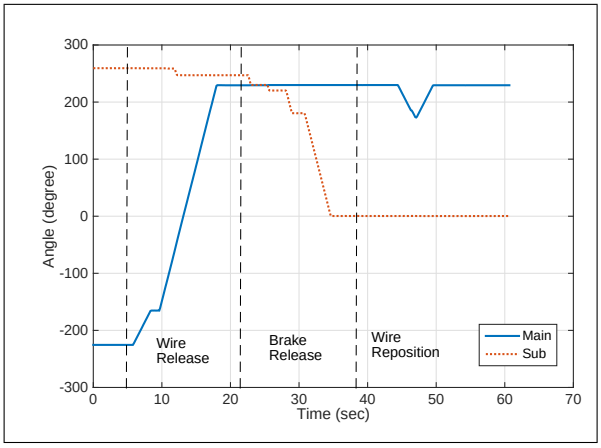

Fig. 17. Position value of two actuators in unlocking process

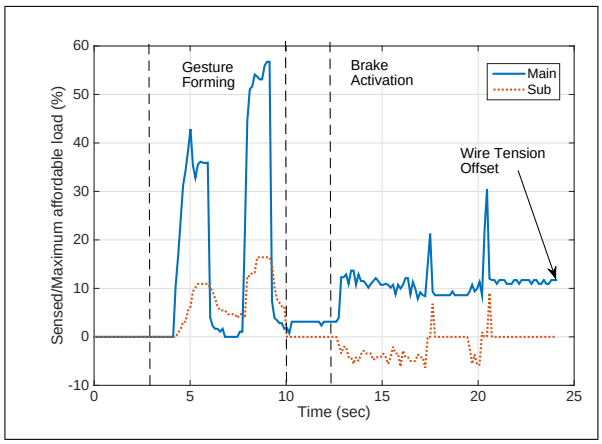

Fig. 16. Sensed load/maximum affordable load of two actuators in grasping locking process

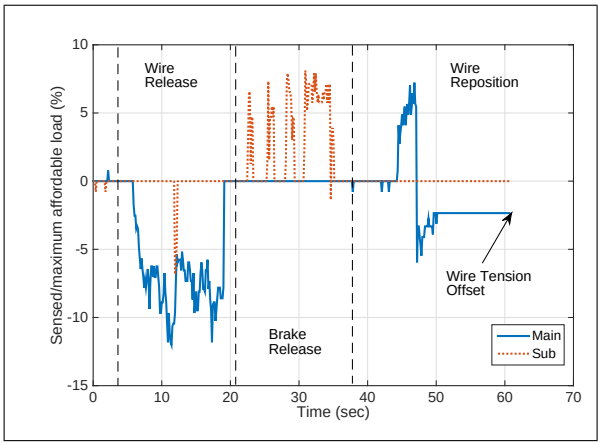

Fig. 18. Sensed load/maximum affordable load of two actuators in unlocking process

and contact force and gives a guideline of the threshold determination. For this object, if we set the threshold to 3Nm, the gripper will be locked after the grasping posture completes, and a certain grasping force is ensured.

A grasping-locking experiment is performed to confirm the operation of SLUM. The experiment is repeated several times with different objects, a demonstration video is attached. The sensed position and load of both main and sub-actuator in whole process is shown in Figs. 15 and 16. In Fig. 15, since we can see the sub-actuator stays still approximately in the posture forming part, we can assume that terminal B of the differential is fixed and the terminal A, which is connected to the wire input of the fingers, rotates in twice the speed of the main actuator. This result corresponds with the fast closing motion of the gripper (posture forming time is about 1.5sec). The little rebound in blue line shows the balance of the actuator torque and the reaction force from the object. After the posture is formed, two actuators rotate synchronously to activate the brake. We applied position control in this state to check the activation of the brake. The terminal A of differential remains in its positon while the terminal B rotates and drives the worm gear and the brake shoe consequently. In Fig. 16, the load of sub-actuator in the posture forming state indicates the torque requirement to prevent terminal B from rotating (which is the purpose of the threshold). The load in the brake activation state is relatively low in comparison with posture forming. The offset of the main actuator in the end of the process indicates the wire tension between the terminal A and the drum. In the demonstration video, we could observe that the main actuator rotates slightly after turning off the power supply due to this wire tension.

The unlocking and position initializing of the gripper is executed after each SLUM experiment. In Fig. 17, we can see that the main actuator rotates reversely to release the wire between the terminal A and the drum. The sub-actuator is turned ‘off’ in this state, the position decreases slightly (terminal B also rotates reversely). Secondly, sub-actuator is turned ‘on’ to release the brake and returns the brake shoe to its initial state. Finally, the main actuator adjusts the tension of the wire. In Fig. 18, the load of the two actuators in the whole unlocking process are also relatively low in comparison with the grasping-locking process.

The payload of the SLUM gripper is also experimentally evaluated. We operate the gripper to grasp a rod with a diameter of 20mm and lock the grasp. Then, a heavy load is connected to the rod that pulls the rod with its own weight

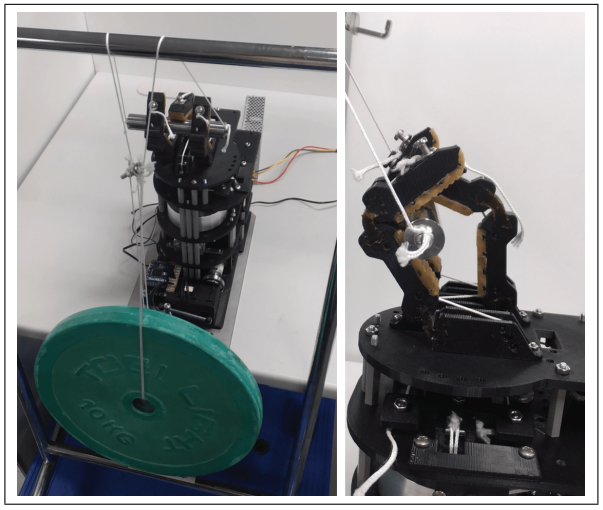

Fig. 19. Evaluation of payload of the SLUM gripper

(the process is executed slowly). In this evaluation, the gripper can afford 10kg weight in most of the experiments (if the grasp posture is not formed appropriately, the grasp may fail). The result of one experiment is shown in Fig. 19. Notice that for our first prototype, the transmission mechanism and the mechanical structure are not optimized. We only use up to 60% power of the actuator to avoid unexpected break. Also, the procedure of the experiment also need improvement to examine the maximum payload.

V. Conclusion

To satisfy the tasks demanding adaptive and firm grasps, we propose a concept called self-locking underactuated mechanism (SLUM). A hardware prototype was designed and built to evaluate the feasibility of this concept. We confirmed that the sequence of the fingers adapting, grasping the object and being locked by the brake has been accomplished successfully. Its capacity of generating the expected payload in a locked posture was also successfully demonstrated for a given object.

As future work, the kinematics of the gripper, including the number of digits, phalanges will be reconsidered to conform with the target applications. Besides adding a mechanism to change the configuration of the fingers, we plan to modularize the underactuated hand with different kinematics. Also, the development of a miniature and efficient brake activating threshold adjuster (BATA), which is possible by applying a smaller sub-actuator and some passive mechanical components, is essential. Finally, the overall size and the orientation of the differential and the locking device needs to be substantially improved.

References

[1] J. Vaillant, A. Kheddar, H. Audren, F. Keith, S. Brossette, A. Escande, K. Bouyarmane, K. Kaneko, M. Morisawa, P. Gergondet, E. Yoshida, S. Kajita and F. Kanehiro, Multi-contact vertical ladder climbing with an HRP-2 humanoid, Autonomous Robots, 40(3), pp.561–580, 2016.

[2] K. Tai, A. El-Sayed, M. Shahriari, M. Biglarbegian and S. Mahmud, State of the Art Robotic Grippers and Applications, Robotics 2016, 5, 11.

[3] F. Rothling, R. Haschke, J. J. Steil and H. Ritter, Platform Portable Anthropomorphic Grasping with the Bielefeld 20-DOF Shadow and 9-DOF TUM Hand, in Intelligent Robots and Systems, 2007 IEEE/RSJ International Conference on. IEEE, pp.2951-2956, 2007.

[4] Robotiq, 3-Finger Adaptive Robot Gripper, [Online]. Available: http://robotiq.com/products/industrial-robot-hand/

[5] L. Birglen, T. Laliberte and C. M. Gosselin, Underactuated Robotic Hands, Springer, 2008.

[6] M. G. Catalano, G. Grioli, E. Farnioli, A. Serio, C. Piazza and A. Bicchi, Adaptive synergies for the design and control of the pisa/iit softhand, International Journal of Robotics Research 2014, pp.768-782, 2014.

[7] K. Telegenov, Y. Tlegenov and A. Shintemirov, An underactuated adaptive 3D printed robotic gripper, on Mecatronics 2014, IEEE, pp.110-115, 2014.

[8] R. R. Ma, L. U. Odhner and A. M. Dollar, A Modular, Open-Source 3D Printed Underactuated Hand, in Robotics and Automation (ICRA), 2013 IEEE International Conference on. IEEE, pp.2737-2743, 2013.

[9] T. Takayama, Y. Chiba and T. Omata, Tokyo-TECH 100 N Hand : Three-fingered eight-DOF hand with a force-magnification mechanism, in Robotics and Automation (ICRA), 2009 IEEE International Conference on. IEEE, pp.593-598, 2009.

[10] M. Plooij, G. Mathijssen, P. Cherelle, D. Lefeber and B. Vanderborght, Review of locking devices used in robotics, IEEE Robotics and Automation Magazine, vol. 22, pp.106-117, 2015.

[11] M. Tavakoli, L. Marques and A. T. de Almeida, Flexirigid, a novel two phase flexible gripper, Intelligent Robots and Systems (IROS), 2013 IEEE/RSJ International Conference on, pp.5046-5051, 2013.

[12] B. Peerdeman, S. Stramigioli, E. E. G. Hekman, D. M. Brouwer and S. Misra, Development of Underactuated Prosthetic Fingers with Joint Locking and Electromyographic Control, Mechanical engineering research, 3, pp130-142. 2013.

[13] M. Controzzi, C. Cipriani and M. C. Carrozza, Miniaturized non-back-drivable mechanism for robotic applications, Mechanism and Machine Theory, vol. 45, Issue 10, pp.1395-1406, 2010.

[14] NAMIKI PRECISION JEWEL CO, Multiple DOF hand with grasp force higher than 50kgf (in Japanese) [Online]. Available: http://www.jst.go.jp/pr/announce/20160307/

[15] A. M. Dollar and R. R. Ma, Yale OpenHand Project, [Online]. Available: https://www.eng.yale.edu/grablab/openhand/

[16] A. M. Dollar and R. D. Howe, Joint coupling design of underactuated hands for unstructured environments, International Journal of Robotics Research 2011, vol. 30, no. 9, pp.1157-1169, 2011.

[17] S. R. Schmid, B. J. Hamrock and B. Jacobson, Fundamentals of Machine Elements, Third Edition, CRC Press, 2013.